

Linear optical response of zinc-blende and wurtzite III-N (III = B, Al, Ga, and In)

C. Persson^{a,*}, A. Ferreira da Silva^b

^aDepartment of Materials Science and Engineering, Royal Institute of Technology, SE-100 44 Stockholm, Sweden

^bInstituto de Física, Universidade Federal da Bahia, Campus de Ondina, 40210 340 Salvador, Bahia, Brazil

Available online 3 April 2007

Abstract

We present calculated dielectric function $\varepsilon(\omega)$ and linear optical absorption $\alpha(\omega)$ of the cubic and hexagonal structures of BN, AlN, GaN, and InN, employing an all-electron linearized augmented plane wave method within the local density approximation (LDA) plus quasi-particle (QP) correction. We show that this LDA+QP approach yields accurate high-frequency dielectric constant $\varepsilon(\infty)$. Moreover, by employing a modelled electron–optical phonon interaction we calculate the static dielectric function $\varepsilon(0)$.

© 2007 Elsevier B.V. All rights reserved.

PACS: 71.20.Nr; 71.38.Fp; 78.20.Bh; 78.20.Ci

Keywords: B1. Nitrides; B2. Semiconducting materials; A1. Computer simulation; A1. Crystal structure

1. Introduction

The III-N semiconductors have superior optical properties for optoelectronic technologies. In this work, we present calculations of the dielectric function $\varepsilon(\omega) = \varepsilon_1(\omega) + i\varepsilon_2(\omega)$ and the absorption coefficient $\alpha(\omega)$ of zinc-blende (zb) T_d^2 and wurtzite (wz) C_{6v}^4 structures of III-N (III = B, Al, Ga, and In) using the fully relativistic, full-potential linearized augmented plane wave (FPLAPW) method [1]. We show that the local density approximation (LDA) plus a quasi-particle (QP) correction yields accurate band-gap energies $E_g(\text{LDA} + \text{QP})$ for all eight III-N structures, as well as accurate high-frequency dielectric constant $\varepsilon(\infty) \equiv \varepsilon(0 \ll \omega \ll E_g/\hbar)$. We also present calculated static dielectric function $\varepsilon(0) \equiv \varepsilon(\omega \rightarrow 0)$, where the electron–phonon interaction is modelled assuming constant longitudinal optical phonon frequency.

2. Electronic structure of III-N

The LDA is well known to underestimate the band-gap energy E_g for most semiconductors, and, for instance, the

discussion of InN band gap is still controversial [2]. In this work we estimate the correction to the LDA band gap by using a QP method proposed by Bechstedt and Del Sole [3].

Table 1
The band-gap energy E_g of zb-III-N obtained from the LDA+QP calculation

		zb-BN	zb-AlN	zb-GaN	zb-InN
CBM.		<i>X</i>	<i>X</i>	Γ	Γ
$E_g + \Delta_g$ (eV)	LDA+QP	6.49	5.11	3.24	0.59
E_g (eV)	Expt.	6.45	5.34	3.2, 3.3	0.5–2.0

References to measured data are found in Ref. [4].

Table 2
The band-gap energy E_g of wz-III-N obtained from the LDA+QP calculation

		wz-BN	wz-AlN	wz-GaN	wz-InN
CBM		<i>K</i>	Γ	Γ	Γ
$E_g + \Delta_g$ (eV)	LDA+QP	7.17	6.05	3.55	0.67
E_g (eV)	Expt.		6.08–6.28	3.50	0.5–2.0

References to measured data are found in [Ref. 4].

*Corresponding author.

E-mail address: clas.persson@mse.kth.se (C. Persson).

We find [4] $E_g(\text{LDA+QP}) = 6.49, 3.24, 5.11,$ and 0.59 eV, for zb BN, GaN, AlN, and InN, respectively, which agree with measured values of 6.45, 3.2–3.3, 5.34 and 0.5–2.0 eV (references are found in Ref. [4]). zb-BN, and zb-AlN have

X-point conduction-band minimum (CBM), whereas zb-GaN and zb-InN have direct Γ -point band gap. Interestingly, the weak spin-orbit interaction in zb-AlN moves valence-band maximum (VBM) from the $\Gamma\text{K} = \Sigma$ -line to

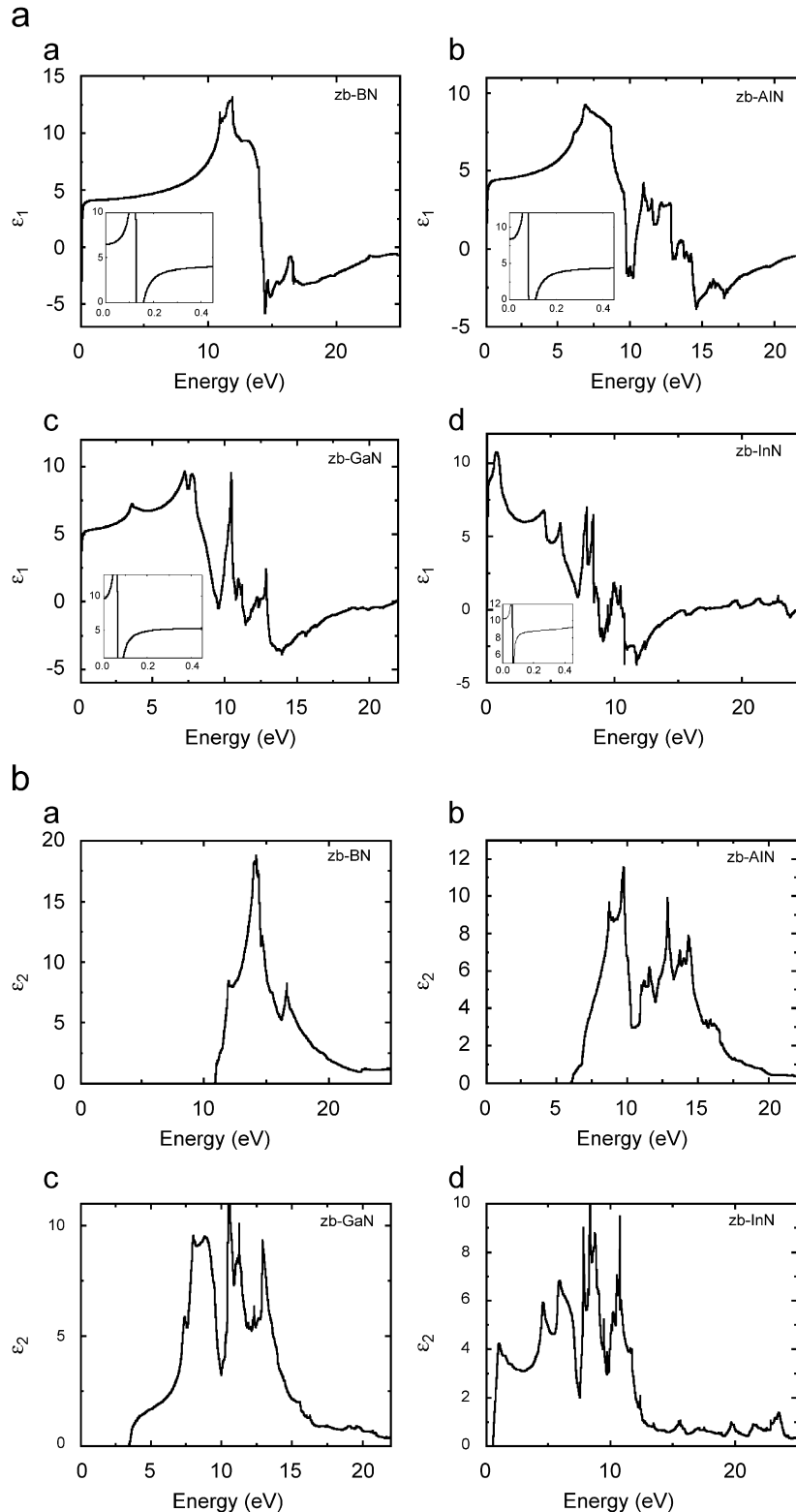


Fig. 1. (a) Real part of the dielectric function of zb-III-N. (b) Imaginary part of the dielectric function of zb-III-N.

the Γ -point. wz-BN has indirect band gap at the K-point CBM, whereas the other wz-III-Ns have direct Γ -point band gaps. LDA+QP yields $E_g(\text{LDA+QP}) = 7.17, 6.05, 3.55\text{eV}$, and 0.67eV for wz BN, AlN, GaN, and InN,

respectively. Experimental values for AlN, GaN and InN are $6.08\text{--}6.28, 3.50,$ and $0.5\text{--}2.0\text{eV}$ [4,5]. In Table 1 and Table 2 we show the results for zb-III N and wz-III N, respectively.

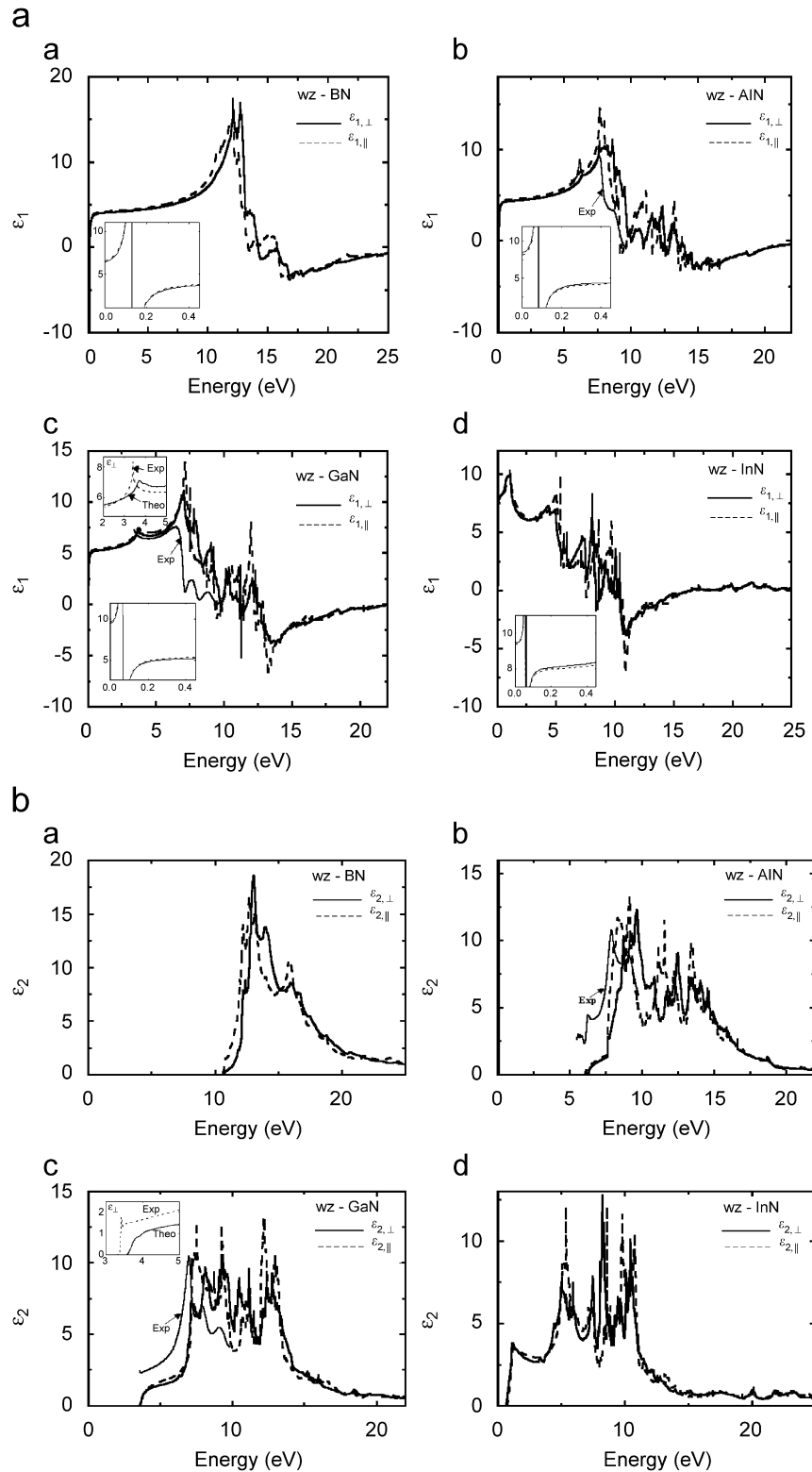


Fig. 2. (a) Real part of the dielectric function of wz-III-N. (b) Imaginary part of the dielectric function of wz-III-N.

3. Linear optical response of III-N

The dielectric function $\varepsilon(\omega)$ of the semiconductors describes the response of the material due to a change in

the charge distribution. The dielectric function is thus an important property for describing the screening of the semiconductor near dopants, defects, and other structural perturbations of the crystal. It has been shown by Del Sole

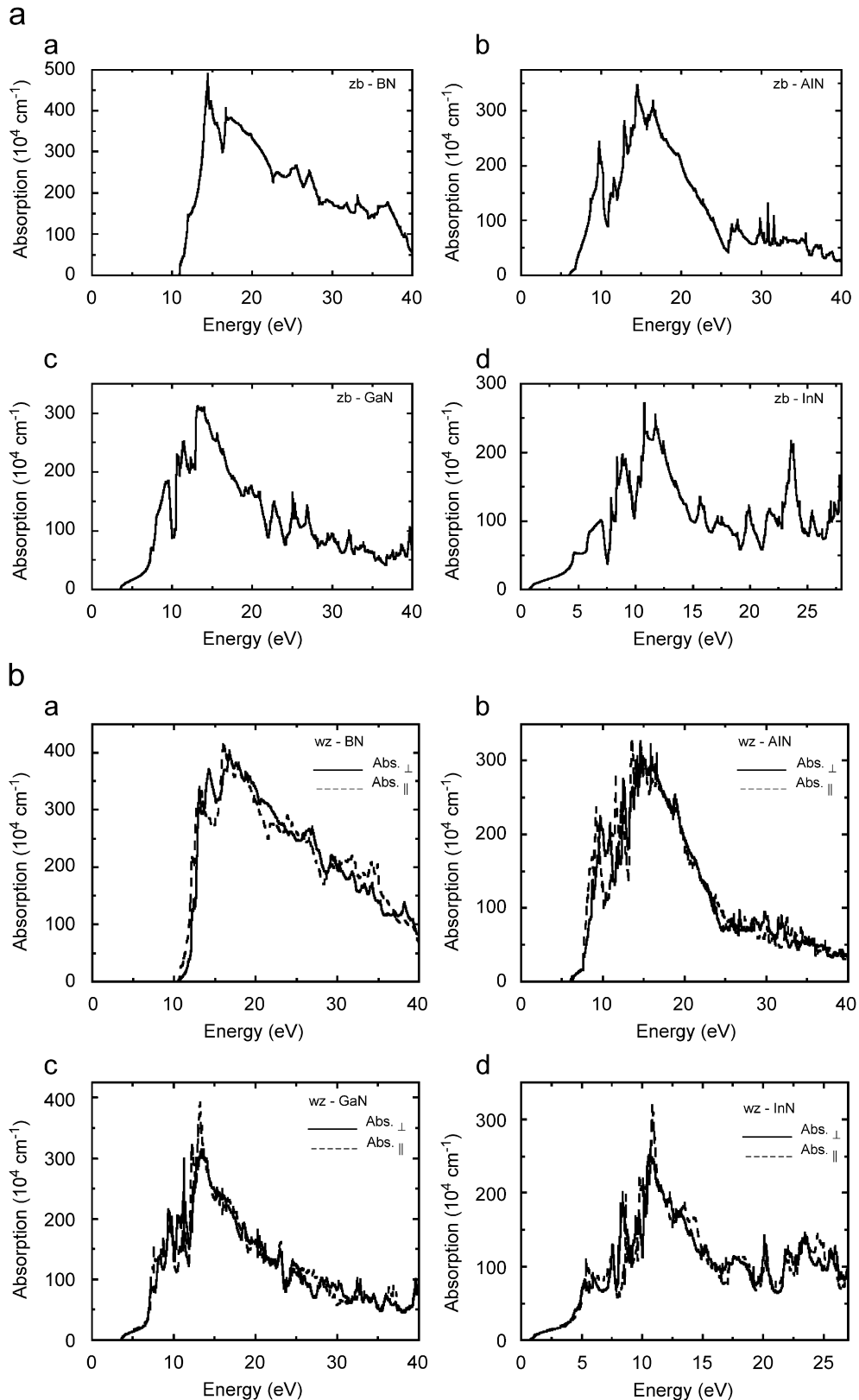


Fig. 3. Absorption coefficients of (a) zb-III-N and (b) wz-III-N.

and Girlanda [6] that the LDA combined with the constant band-gap correction describes the band structure rather well.

Within the linear response theory the dielectric function in the long wave length limit ($|\mathbf{k}-\mathbf{k}'| = \mathbf{0}$) is calculated directly from the electronic structure via the joint density-of-states and the optical matrix elements [4]:

$$\begin{aligned} \varepsilon_2^{xy}(\omega) = & \frac{4\pi^2 e^2}{\Omega m_0^2 \omega^2} \sum_{\mathbf{k}, j, j', \sigma} \langle \mathbf{k}, j, \sigma | \hat{p}_x | \mathbf{k}, j', \sigma \rangle \\ & \times \langle \mathbf{k}, j', \sigma | \hat{p}_y | \mathbf{k}, j, \sigma \rangle f_{\mathbf{k}j}(1 - f_{\mathbf{k}j'}) \\ & \times (E_{j'}(\mathbf{k}) - E_j(\mathbf{k}) - \hbar\omega). \end{aligned} \quad (1)$$

Here, $f_{\mathbf{k}j}$ is the Fermi distribution function. The real part of the dielectric function is obtained from the Kramers–Kronig transformation relation:

$$\varepsilon_1(\omega) = 1 + \frac{1}{2\pi} \int_0^\infty d\omega' \varepsilon_2(\omega') \left(\frac{1}{\omega' - \omega} + \frac{1}{\omega' + \omega} \right). \quad (2)$$

The electronic structure calculations do not include electron–phonon interactions. However, in polar semiconductors the optical phonons play an important role for the low-frequency dielectric function. The low-frequency $\varepsilon(\omega \approx 0)$ dielectric constant of polar materials can only be determined by considering the phonon screening. We approximate this electron–optical phonon (ep) interaction by using a delta function in $\varepsilon_2(\omega)$ at the transverse phonon frequency ω_{TO} assuming constant optical phonon frequency distribution. For the optical phonon energies, we used the experimental values (see Ref. [4] for details): $\hbar\omega_{\text{TO}} = 130.8, 82.7, 66.0,$ and 59.3 meV and $\hbar\omega_{\text{LO}} = 161.8, 112.8, 88.0,$ and 86.0 meV in wz BN, AlN, GaN, and InN, respectively. We assume the same values for the zb structures:

$$\varepsilon_2^{\text{ep}}(\omega) = \delta(\omega - \omega_{\text{TO}}) \pi \varepsilon_1(\infty) \frac{(\omega_{\text{LO}}^2 - \omega_{\text{TO}}^2)}{2\omega_{\text{TO}}}. \quad (3)$$

To calculate the contribution to the dielectric function due to this electron–phonon interaction, the experimental values of the two phonon frequencies ω_{TO} and ω_{LO} are employed. We apply the LDA+QP+ep approach for calculating (Figs. 1–3) the linear optical response of III-N. We assume same values of the frequencies for both wz and zb structures. Figs. 1a and 2a display the calculated real part of the dielectric function of zb- and wz-III-N respectively. In Figs. 1b and 2b we show the calculated imaginary part of the dielectric function of zb- and wz-III-N, respectively. Figs. 3a and 3b display the absorption coefficient of zb- and wz-III-N, respectively.

In Table 3, we present the calculated dielectric constants of intrinsic zb- and wz-III-N using the LDA+QP+ep approach. For comparison we also present the results for the LDA+ep calculation (in brackets) without the band-gap correction. By adding the ep-interaction to $\varepsilon_2(\omega)$, and thereafter calculating $\varepsilon_1(\omega)$ through the Kramers–Kronig dispersion relation, we obtain a more realistic static

Table 3

The dielectric constants of III-N obtained from the LDA+QP+ep calculation

		$\varepsilon(0)$ Calc.	$\varepsilon(\infty)$ Calc.	$\varepsilon(0)$ Expt.	$\varepsilon(\infty)$ Expt.
zb-BN	ε	6.45 (7.23)	4.14 (4.67)	7.1	4.5
zb-AlN	ε	8.35 (9.26)	4.46 (5.24)		
zb-GaN	ε	9.56 (10.73)	5.32 (6.12)		5.29, 5.3
zb-InN	ε	10.24 (15.10)	8.88 (12.91)		
wz-BN	ε_\perp	6.40 (7.17)	4.11 (4.63)		4.95
	ε_\parallel	6.54 (7.41)	4.22 (4.80)		4.1
wz-AlN	ε_\perp	8.19 (9.02)	4.37 (5.10)	8.5	4.68, 4.14
	ε_\parallel	8.49 (9.44)	4.54 (5.32)		4.84, 4.32
wz-GaN	ε_\perp	9.50 (10.59)	5.26 (6.09)	8.9, 9.5	5.35, 5.14
	ε_\parallel	9.69 (10.88)	5.38 (6.24)		5.31, 5.31
wz-InN	ε_\perp	9.51 (14.00)	8.21 (11.63)	8.1, 15.3	9.3, 8.4
	ε_\parallel	9.41 (13.87)	8.11 (11.51)		

The values in brackets represent the LDA+ep calculations. References to measured data are found in Ref. [4].

dielectric constant. Early LDA calculations of the high-frequency dielectric constants of zb- and wz-III-N by Christensen and Corczyca [7] yielded $\varepsilon(\infty) = 4.14, 3.90, 4.78, 6.15$ in zb BN, AlN, and GaN, InN respectively, obtained from a linear muffin-tin orbital ASA calculation with the underestimate LDA band-gap energies. LDA pseudopotential calculations (including a local field corrections) of the high-frequency $\varepsilon(\infty)$ dielectric function of zb- and wz-III-N by Karch and Bechstedt [8] ($\varepsilon(\infty) = 4.54, 4.46,$ and 5.41 in zb BN, AlN, and GaN, respectively) yield similar results as the present values. It is worthwhile to point out that we have calculated the crystal-field split-off energy for wz-AlN, in the absence of spin–orbit interaction, of the uppermost valence bands given a value of $|\Delta_{\text{cf}}| = 212$ meV [9], a value very close to the recently reported experimental values 225 meV [5] and 230 meV [10] respectively. It is worth to point out that wz-AlN, in contrast to wz-BN, wz-GaN and wz-InN [4], has a negative crystal-field splitting energy which means that the double degenerate Γ_5 state is energetically above the single degenerate Γ_1 state. Here Γ_α is the single-group representation of the irreducible representation.

4. Summary

In conclusion, we present a calculation of the electronic band structure and the dielectric constants for intrinsic zincblende and wurtzite nitrides, which are important for the understanding of the electronic transport properties in these semiconductors. We show that the LDA+QP+ep approach yields accurate band-gap energies, dielectric functions and absorption. The QP band-gap correction does however not improve the LDA energy-band dispersion.

Acknowledgments

This work was supported by the Swedish Research Council (VR), Brazilian National Research Council

(CNPq), FAPESB (Bahia/Brazil), CNPq/REMAN and The Swedish Foundation for International Cooperation in Research and Higher Education (STINT).

References

- [1] P. Blaha et al., WIEN95, Technical University of Vienna 1995. [Improved and updated version of copyrighted WIEN-code, which was published by P. Blaha et al., *Comput. Phys. Commun.* 59 (1990) 399].
- [2] C. Trager-Cowan, *Phys. Stat. Sol. (c)* 2 (2005) 2240.
- [3] F. Bechstedt, R. Del Sole, *Phys. Rev B* 38 (1998) 7710.
- [4] C. Persson, A. Ferreira da Silva, in: M. Razeghi, M. Henini (Eds.), *Optoelectronic Devices: III-Nitrides*, Elsevier Advanced Technology, London, 2004, pp. 479–559, ISBN:0-08-044426-1.
- [5] E. Silveira, J.A. Freitas Jr., O.J. Glembocki, G.A. Slack, L.J. Schowalter, *Phys. Rev. B* 71 (2005) R041201.
- [6] R. Del Sole, R. Girlanda, *Phys Rev B* 48 (1993) 11789.
- [7] N.E. Christensen, I. Corczyca, *Phys Rev. B* 50 (1994) 4397.
- [8] K. Karch, F. Bechstedt, *Phys. Rev. B* 57 (1998) 7043.
- [9] A. Ferreira da Silva, N. Souza Dantas, J.S. Almeida, R. Ahuja, C. Persson, *J. Crystal Growth* 281 (2005) 151.
- [10] L. Chen, B.J. Skromme, R.F. Dalmau, R. Schlessler, Z. Sitar, C. Chen, W. Sun, J. Yang, M.A. Khan, M.L. Nakarmi, J.Y. Lin, H.X. Jiang, *Appl. Phys. Lett.* 85 (2004) 4334.